A Novel Active Inductor and Its Application to Inductance-Controlled Oscillator

Yong-Ho Cho, *Associate Member, IEEE,* Song-Cheol Hong, *Member, IEEE,* and Young-Se Kwon, *Member, IEEE*

***Abstract*—This paper describes a novel active inductor using a common-source cascode FET with an inductive feedback. A compact lossy active inductor, which consists of a common-source FET and a feedback resistor, was used as the feedback inductor to achieve high Q-factor and tunability, as well as reduce the chip size. The fabricated active inductor achieved more than 100 Q-factors with the maximum value of 3400 over the frequency range of 200 MHz, in the vicinity of 1.7 GHz. Inductance was tuned from 9.6 to 56 nH at 1.7 GHz by the variation of the feedback resistance of the lossy active inductor. Using this active inductor (as a frequency-selective element in the resonator), a monolithic inductance-controlled FET oscillator was fabricated, which demonstrated an 18% frequency-tuning range from 1.73 to 2.07 GHz, with an output power range from −9.3 to −6.3 dBm.**

***Index Terms*—Active inductor, MMIC, oscillator.**

I. Introduction

SPIRAL inductors have been widely used in GaAs monolithic microwave integrated circuits (MMIC's) due to their simple planar structure, wide dynamic range, and no dc power consumption. However, their conductive losses make it difficult to apply them to the high-performance *L–C* resonators of microwave filters and oscillators. To overcome this problem, a large amount of research, which introduced high-Q or negative-resistance active inductors in the resonators, has been done [1]-[9].

As an approach for the microwave active inductor, Hara *et al*. reported a very simple active inductor using a common-source cascode FET with a resistive feedback [3]. It was successfully implemented in the broad-band amplifier. However, because of its high series resistance, the active inductor is limited in its application to MMIC's. The resistive feedback topology was later changed to either the common-gate FET or the common-gate cascode-FET feedback topology [4], [5]. For these two topologies, the series resistance of the active inductor was significantly reduced.

For the tunable active-filter design, a high-Q tunable active inductor was demonstrated [7]. To realize tunability, a variable resistor was employed in the common-gate FET feedback loop of the common-source cascode FET. High Q-factor was achieved by the introduction of a shunt resistor between the gate of the feedback FET and ground. The feedback FET with the shunt resistor produced a negative resistance and controlled the level of series resistance. However, a low-voltage operation is difficult in the common-source cascode-FET inductor with the common-gate FET or common-gate cascode-FET feedback because four or five FET's with the same size, including a biasing transistor, must be stacked.

In other approaches, active inductors were realized with the negative resistance technique, where an inductance was employed in the feedback loop of a common-base bipolar transistor (BJT) [1], [2] or a common-gate FET [6] to generate negative resistance and compensate for the loss of the inductor. These active inductors have very simple topology, which is composed of a transistor and a feedback inductor. However, bandpass filters using these approaches resulted in large chip size due to large spiral feedback inductors [1], [6]. For the case of the common-gate FET inductor [6], the integration of varactor diodes is required for center-frequency tuning.

In the authors' previous paper [10], a new active inductor was proposed, in which, instead of a large spiral inductor, a compact lossy active inductor composed of a common-source FET and a feedback resistor was introduced in the feedback loop of a common-source cascode FET to achieve high Q-factor and tunability. Its performances were demonstrated through circuit simulation and it was applied to the design of the monolithic oscillator. In this paper, the design and measured results of the new active inductor are discussed. In addition, an inductance-controlled oscillator, which incorporates this new active inductor in the oscillator resonator, is demonstrated.

II. Inductor Design

A common-source FET with a resistive feedback is a very simple active inductor, as shown in Fig. 1(a). When the FET is assumed to be composed of transconductance g_m gate-to-source capacitance $C_{\rm gs}$ and gate-to-drain capacitance $C_{\rm gd}$, the output impedance Z of the active inductor is given by

$$Z = \frac{1 + j\omega R_f(C_{\rm gs} + C_{\rm gd})}{g_m - \omega^2 R_f C_{\rm gs} C_{\rm gd} + j\omega(C_{\rm gs} + g_m R_f C_{\rm gd})}. \quad (1)$$

At low frequency, the series resistance of the active inductor can be approximated by the reciprocal of the transconductance of the FET and the inductance by the feedback resistance divided by the radian-current cutoff frequency ω_T, of the FET. To reduce series resistance in this active inductor, a wide-gatewidth FET is required because the transconductance is proportional to the gatewidth. However, the Q-factor of the inductor can not be significantly improved by just increasing the gatewidth because of the conductive losses and other parasitics which are not considered in this analysis. In addition,

Manuscript received October 14, 1996; revised April 25, 1997.

The authors are with the Department of Electrical Engineering, Korea Advanced Institute of Science and Technology (KAIST), Taejon, 305-701 Korea.

Publisher Item Identifier S 0018-9480(97)05376-3.

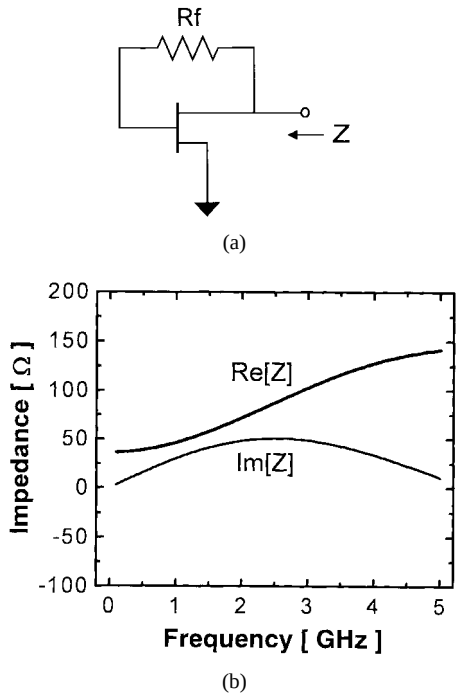

Fig. 1. A simple lossy active inductor using a common-source FET with a resistive feedback. (a) Circuit schematic. (b) Simulated results.

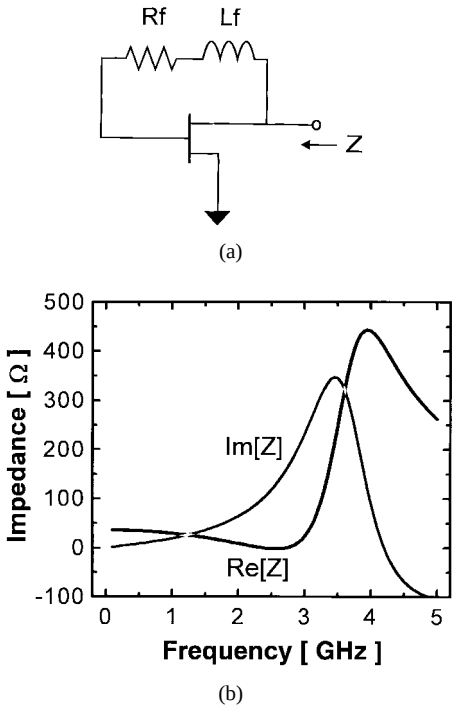

Fig. 2. The proposed high-Q active inductor using a common-source FET with an inductive and resistive feedback. (a) Circuit schematic. (b) Simulated results.

the operating dc power consumption of a wide-gatewidth FET is high. Simulated results of the active inductor composed of a 200-μm common-source FET with 1-μm gatelength and a feedback resistance of 500 Ω is shown in Fig. 1(b). The full small-signal equivalent circuit model of the FET was used. It is shown that the Q-factor is less than 1 throughout the frequency range.

A simple method reducing the series resistance of the active inductor by the introduction of an inductance in the resistive feedback loop of the common-source FET is proposed. The newly proposed active inductor is shown in Fig. 2(a). If R_f is replaced with $R_f + j\omega L_f$ in (1), one can expect the real part of Z to be zero or negative around the resonant frequency of L_f and $C_{\rm gs}+C_{\rm gd}$. After further manipulation of (1), one finds that the output impedance Z of the active inductor shown in Fig. 2(a) is given by $\mathrm{Re}[Z]$ and $\mathrm{Im}[Z]$, shown in (2) and (3) at the bottom of the page, where

$$\omega_{r1} = 1/\sqrt{L_f(C_{\rm gs}+C_{\rm gd})} \tag{4}$$

$$\omega_{r2} = 1/\sqrt{L_f C_{\rm gd}} \tag{5}$$

$$\omega_{t1} = g_m/(C_{\rm gs}+C_{\rm gd}) \tag{6}$$

$$\omega_{t2} = g_m/C_{\rm gs} \tag{7}$$

$$\omega_{r1} = 1/(R_f C_{\rm gd}). \tag{8}$$

In the frequency range of ω where $\omega_{r1} < \omega < \omega_{r2}$, $1-\omega^2/\omega_{r1}^2$ becomes negative and $1-\omega^2/\omega_{r2}^2$ becomes positive so that the resistance of the inductor can be zero or negative, and the inductance can be higher than that of the only resistance feedback inductor depending on ω_{ri}, ω_{ti} and ω_f. Simulation results of the active inductor which consists of a 200-μm common-source FET, a feedback resistance of 250 Ω, and a feedback inductance of 25 nH is shown in Fig. 2(b). The series resistance of the inductor is significantly reduced in the frequency range from 2 to 3 GHz.

In the circuit simulation, it was found that the feedback inductance must be, at least, several tens of nanohenrys to achieve zero or negative output resistance. The realization of such a high inductance with a spiral inductor requires a large wafer space and is difficult in microwave frequency due to the parasitic capacitance. Fortunately, this high inductance can be easily achieved consuming a compact wafer area by incorporating a common-source FET with high feedback resistance. The inductance value of the resistive feedback inductor is proportional to the feedback resistance [see (1)]. Replacing the inductive and resistive feedback elements (L_f and R_f) in Fig. 2(a) with this lossy active inductor (a common-source FET with a resistive feedback), one can not only

$$\mathrm{Re}[Z] = \frac{(1-\omega^2/\omega_{r1}^2)(1-\omega^2/\omega_{r2}^2)/g_m + (\omega^2/\omega_{t2}^2 + \omega^2/\omega_{t1}\omega_f)R_f}{(1-\omega^2/\omega_{t2}\omega_f - \omega^2/\omega_{r2}^2)^2 + (\omega/\omega_{t2} + \omega/\omega_f - \omega^3/\omega_{r2}^2\omega_{t2})^2} \tag{2}$$

$$\mathrm{Im}[Z] = \frac{\omega R_f}{\omega_{t2}} \cdot \frac{1-\omega^2/\omega_{t1}\omega_f - (1-\omega^2/\omega_{r1}^2)(1-\omega^2/\omega_{r2}^2)/g_m R_f}{(1-\omega^2/\omega_{t2}\omega_f - \omega^2/\omega_{r2}^2)^2 + (\omega/\omega_{t2} + \omega/\omega_f - \omega^3/\omega_{r2}^2\omega_{t2})^2} \tag{3}$$

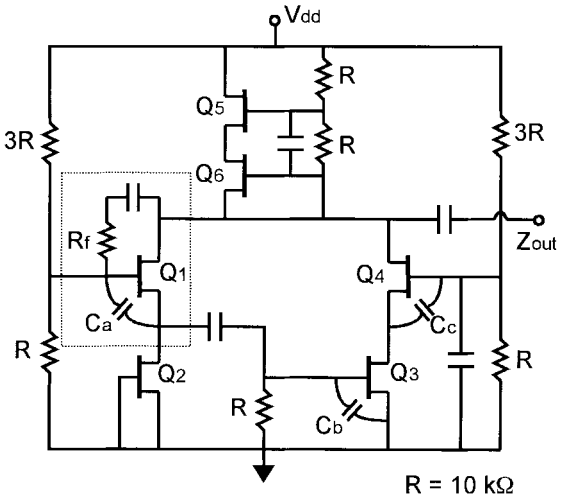

Fig. 3. The full circuit diagram of the proposed active inductor.

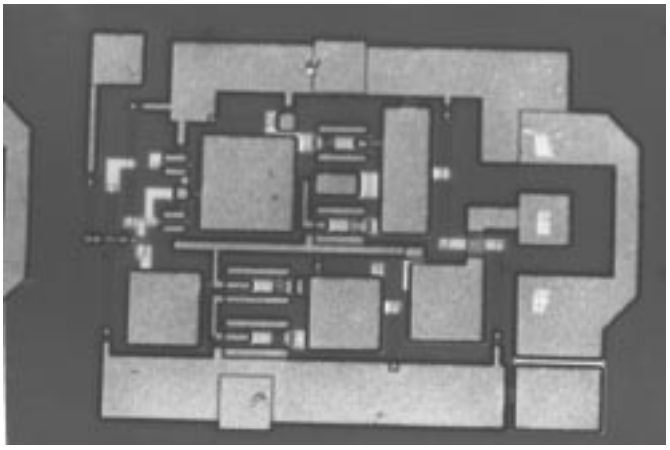

Fig. 4. Photograph of the fabricated active inductor. Chip size is 0.9 × 0.7 mm^2 including bias pads and on-wafer measurement pads.

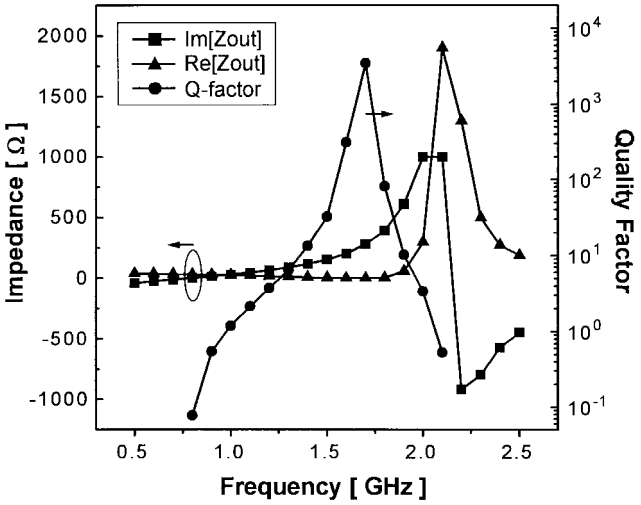

Fig. 5. Measured output reactance, resistance, and Q-factor of the active inductor at $V_{dd} = 9$ V and $I_{dd} = 41$ mA.

reduce the required wafer space, but also achieve the easy tunability of inductance. If the feedback resistance of the lossy active inductor is changed, the output inductance is varied according to (3) because the output impedance of the lossy active inductor is dependent on the feedback resistance.

The full circuit diagram of the proposed active inductor is shown in Fig. 3. Capacitors C_a, C_b, and C_c are external gate-to-source capacitors for operating frequency tuning and other capacitors are dc-blocking capacitors. Resistors other than R_f are used as biasing resistors. A 250-μm cascode FET (Q_5 and Q_6) was used for the active biasing circuit to increase the output impedance. For a low-voltage operation, the active biasing circuit can be replaced with a passive biasing circuit, such as a choke inductor. Instead of the common-source FET used in the analysis of the active inductor, a 200-μm common-source cascode FET (Q_3 and Q_4) was implemented as a main transistor because it has higher $g_m R_{\rm ds}$ than that of a common-source FET. The relatively low drain-to-source output resistance of the FET is the main cause of increasing the series resistance of the FET active inductor. The dashed box in Fig. 3 indicates the lossy active inductor used as an inductive and resistive feedback element of the common-source cascode FET. It consists of a 50-μm FET and a feedback resistor R_f. To achieve a tunable active inductor, the resistor R_f is replaced with a variable resistor. The variable resistor is easily realized with a cold FET by controlling the gate bias voltage.

III. Experimental Results

The designed circuits were fabricated in the authors' laboratory. An epitaxial wafer grown by molecular beam epitaxy (MBE) was the starting substrate. The formation of AuGe/Ni/Au ohmic contact was followed by the mesa etching for the device isolation. Nominal 1-μm gates were defined using an optical contact lithography technique. Recessed gate FET's showed the saturation current of 180 mA/mm, the transconductance of 135 mS/mm and the current cutoff frequency of 12 GHz. Resistors were made by either thin NiCr film with the sheet resistance of 20 Ω per square or etched mesa with the sheet resistance of 20 Ω per square. Silicon nitride was deposited for the dielectric film of metal–insulator–metaL (MIM) capacitors and the passivation layer. Each device was connected by gold-plated metal lines. Via hole process was avoided to increase area efficiency and process yield. The fabricated active inductor is shown in Fig. 4. Chip size is about 0.9 × 0.7 mm^2 including biasing pads and on-wafer measurement pads.

The measured performances of the active inductor designed for the fixed inductance is shown in Fig. 5. The measurement was performed at the bias point optimized to achieve high Q-factor. At 1.7 GHz, Q-factor greater than 3400 was achieved, and at that point the measured inductance value was 26 nH. Q-factor was more than 100 over the frequency range of 200 MHz in the vicinity of 1.7 GHz. The bias voltage was as high as 9 V and the bias current was 41 mA. When the active inductor utilized an external-bias choke inductor instead of the internal active-biasing circuit, the operating bias voltage became 5 V.

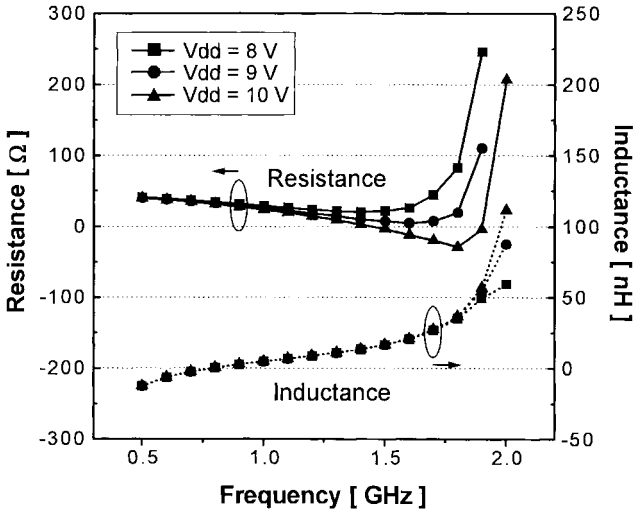

Fig. 6. Measured output impedance characteristics with the bias voltage (V_{dd}) change. As the bias voltage increases from 8 to 10 V, the output resistance decreases from 44 to -20 Ω with the 2% inductance variation at 1.7 GHz.

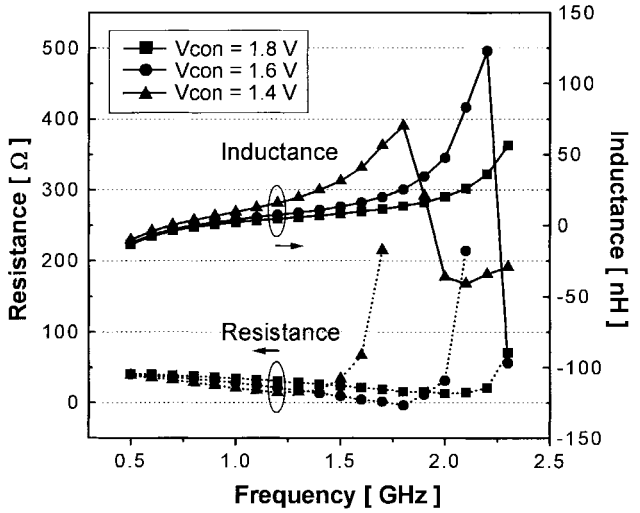

Fig. 7. Measured inductance tuning characteristics of the active inductor. As the control voltage ($V_{\rm con}$) of the variable resistor decreases from 1.8 to 1.4 V, the output inductance increases from 9.6 to 56 nH at 1.7 GHz.

Output resistance of the active inductor was dependent on the bias voltage (V_{dd}). Fig. 6 shows the bias-dependent output impedance. As the bias voltage increased, output resistance of the active inductor decreased or even became a negative value. This is due to the increase of drain-to-source output resistance of the FET with increasing drain-to-source voltage. In comparison with the resistance change, inductance variation was negligible. At 1.7 GHz, the variation was less than 2% while the output resistance variation was between 44 and -20 Ω.

For the tunable active inductor, the feedback resistance of the lossy active inductor was substituted with a cold FET (a variable resistor). The inductance tuning characteristics is shown in Fig. 7. As the gate control voltage ($V_{\rm con}$) of the cold FET decreased, the output inductance increased due to the increase of the feedback inductance and resistance of the common-source cascode FET. A large inductance change from

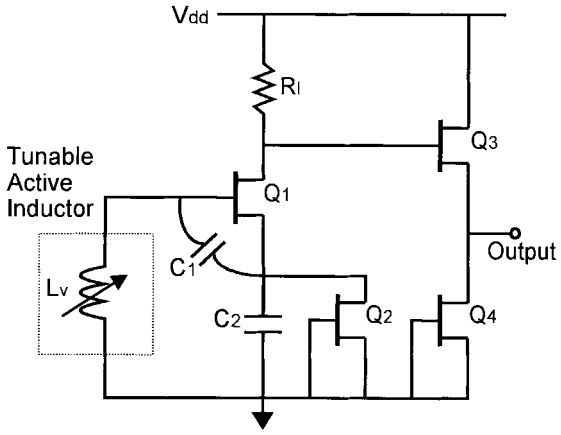

Fig. 8. The circuit diagram of the inductance-controlled oscillator.

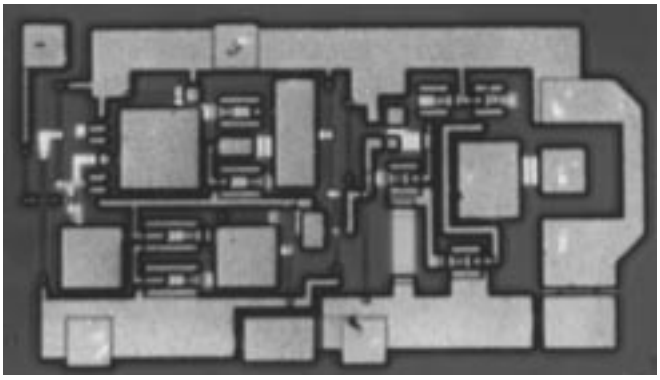

Fig. 9. Photograph of the fabricated inductance-controlled oscillator. Chip size is 1.2 × 0.7 mm^2.

9.6 to 56 nH was occurred at 1.7 GHz. In effect, the series resistance was varied with the gate-control voltage variation. However, it should be noted that the series resistance can be controlled by the bias voltage with negligible inductance variation as shown in Fig. 6.

IV. Application to Inductance-Controlled Oscillator

The proposed tunable active inductor can be applied to realizing narrowband tunable active filters and inductance-controlled oscillators. Compared with the varactor diode capacitor, the tunable active inductor has a wider frequency-tuning capability because it has a wide tuning range of resistance as well as inductance. Also, it can be easily integrated with other FET MMIC circuits because it consists of conventional MMIC components. Until now, active inductors have been principally applied to the monolithic active filters, which have been the main issues in the MMIC applications. As a new application of FET active inductors, a monolithic inductance-controlled oscillator was briefly discussed in [5] but has not been demonstrated.

As shown in Fig. 8, a tunable active inductor (L_v) is implemented in the resonator of oscillator as a frequency-selective element. Compared to the conventional varator-controlled oscillator where the oscillation frequency is tuned

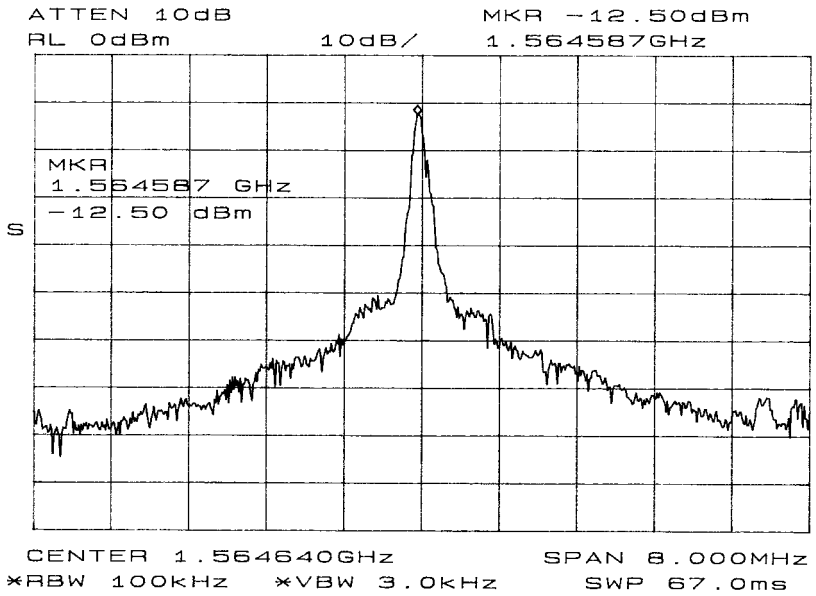

Fig. 10. Output spectrum of the 1.56 GHz fixed-frequency oscillator.

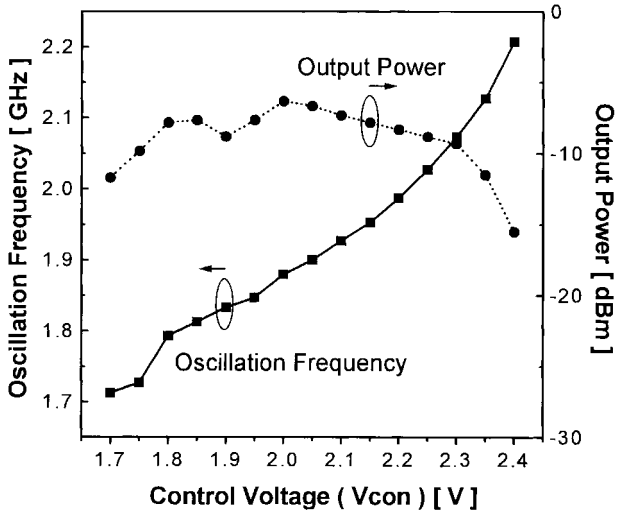

Fig. 11. Measured tuning performances of the inductance-controlled oscillator.

by the varactor capacitance, oscillation frequency is controlled by the inductance of L_v in this oscillator. The oscillator circuit is equivalent to the conventional Colpitts configuration. Transistor Q_1 and capacitor C_2 provides a negative resistance at the gate of Q_1 with a proper drain–load termination. Capacitor C_1 is an external gate-to-source capacitor, which makes the reactance at the gate of Q_1 insensitive to the bias changes. In this paper's design, no spiral inductor was used in order to avoid increasing the chip size. The drain bias voltage of Q_1 was provided through the resistor R_l. Transistor Q_2 was used as a current source. To reduce the loading effect, a source-follower buffer (Q_3 and Q_4) with 50-Ω output resistance was implemented. Fig. 9 shows the fabricated oscillator in a compact chip size of 1.2×0.7 mm^2.

As a test circuit, a fixed-frequency oscillator was also realized by the substitution of the tunable active inductor with a fixed active inductor in the resonator. The output spectrum of the oscillator is shown in Fig. 10. The measurement was performed by HP8564E spectrum analyzer using a microwave on-wafer probe. Bias voltage of the active inductor was 12 V and bias voltage of the oscillator was 8 V. The oscillation frequency was determined to 1.56 GHz with the output power of −12.5 dBm. The phase noises were estimated approximately at −65 dBC/Hz and −100 dBC/Hz at the offset frequency of 100 kHz and 1 MHz from the carrier, respectively. In the case of the unbuffered oscillator, the oscillation frequency was 1.6 GHz and the output power was 3.17 dBm. The phase noise was approximately −90 dBC/Hz at the 1-MHz offset frequency from the carrier.

The tuning performances of the inductance-controlled oscillator is shown in Fig. 11. An 18% frequency-tuning range from 1.73 to 2.07 GHz was achieved and the output power varied from −9.3 to −6.3 dBm in the frequency-tuning range. The oscillator showed relatively poor phase-noise performances. This may be due to the large number of FET's used in the circuits.

V. Conclusion

A new high-Q active inductor for L- and S-band MMIC applications has been developed. The new active inductor utilized a lossy active inductor as a feedback element of a common-source cascode FET to achieve high Q-factor and tunability as well as reduce the chip size. Simplified analytical expressions for the output impedance of the new active inductor were obtained and the predicted results agreed well with the experimental results. The bias-dependent output impedance characteristics and the inductance tuning performance were also examined experimentally. To demonstrate the application of this active inductor to MMIC's, an inductance-controlled FET oscillator was fabricated, which incorporated the active inductor in the oscillator resonator.

REFERENCES

[1] D. K. Adams and R. Y. C. Ho, "Active filters for UHF and microwave frequencies," *IEEE Trans. Microwave Theory Tech.*, vol. MTT-17, pp. 662–670, Sept. 1969.

[2] R. V. Snyder, Jr. and D. L. Bozarth, "Analysis and design of a microwave transistor active filter," *IEEE Trans. Microwave Theory Tech.*, vol. MTT-18, pp. 2–9, Jan. 1970.

[3] S. Hara, T. Tokumitsu, T. Tanaka, and M. Aikawa, "Broad-band monolithic microwave active inductor and its application to miniaturized wide-band amplifiers," *IEEE Trans. Microwave Theory Tech.*, vol. 36, pp. 1920–1924, Dec. 1988.

[4] ———, "Lossless broad-band monolithic microwave active inductors," *IEEE Trans. Microwave Theory Tech.*, vol. 37, pp. 1979–1984, Dec. 1989.

[5] P. Alinikula, R. Kaunisto, and K. Stadius, "Monolithic active resonators for wireless applications," in *IEEE Microwave and Millimeter-Wave Monolithic Circuit Symp. Dig.*, San Diego, CA, May 1994, pp. 197–200.

[6] B. P. Hopf, I. Wolff, and M. Guglielmi, "Coplanar MMIC active band-pass filters using negative resistance circuits," *IEEE Trans. Microwave Theory Tech.*, vol. 42, pp. 2598–2602, Dec. 1994.

[7] S. Lucyszyn and I. D. Robertson, "Monolithic narrow-band filter using ultrahigh-Q tunable active inductors," *IEEE Trans. Microwave Theory Tech.*, vol. 42, pp. 2617–2622, Dec. 1994.

[8] G. F. Zhang and J. L. Gautier, "Broad-band, lossless monolithic microwave active floating inductor," *IEEE Microwave Guided Wave Lett.*, vol. 3, pp. 98–100, Apr. 1993.

[9] S. E. Khoury, "The design of active floating positive and negative inductors in MMIC technology," *IEEE Microwave Guided Wave Lett.*, vol. 5, pp. 321–323, Oct. 1995.

[10] Y. H. Cho, S. C. Hong, and Y. S. Kwon, "Monolithic VCO using a novel active inductor," in *IEEE Microwave and Millimeter-Wave Monolithic Circuit Symp. Dig.*, San Francisco, CA, June 1996, pp. 155–158.

Yong-Ho Cho (A'96) was born in Kangjin, Korea, in 1969. He received the B.S. and M.S. degrees in electrical engineering from the Korea Advanced Institute of Science and Technology (KAIST), Taejon, Korea, in 1992 and 1994, respectively. He is currently working toward the Ph.D. degree at KAIST.

His research interests include GaAs microwave devices and MMIC's for wireless communication applications, and microwave integrated-circuit process technology.

Song-Cheol Hong (S'87–M'88) was born in Korea in 1959. He received the B.S. and M.S. degrees in electronics from Seoul National University, Seoul, Korea, in 1982 and 1984, respectively, and the Ph.D. degree in electrical engineering from the University of Michigan, Ann Arbor, in 1989.

He is currently an Associate Professor in the Department of Electrical Engineering at the Korea Advanced Institute of Science and Technology (KAIST), Taejon, Korea. His research interests are optoelectronic and optomechanical devices, high-speed IC's, and quantum-effect devices.

Young-Se Kwon (S'75–M'76) received the B.S. degree from Seoul National University, Seoul, Korea, in 1968, the M.S. degree from Ohio University, Athens, in 1972, and the Ph.D. degree from the University of California, Berkeley, in 1977, all in electrical engineering.

From 1977 to 1979, he was a Research Associate in the Department of Electrical Engineering, Duke University, Durham, NC. He joined the Department of Electrical Engineering at the Korea Advanced Institute of Science and Technology (KAIST), Taejon, Korea, in 1979, first as an Assistant Professor, and currently as a full Professor. His main research have been focused on the development of AlGaAs/GaAs-based opto-electronic integrated circuits (OEIC). His recent interest includes the development of MMIC's using standard GaAs MESFET and FECFET technology.